JNeurosci Accepted Manuscript

JNeurosci
THE JOURNAL OF NEUROSCIENCE

Research Articles: Systems/Circuits

The origin of GnRH pulse generation: An integrative mathematical-experimental approach

https://doi.org/10.1523/JNEUROSCI.0828-19.2019

Cite as: J. Neurosci 2019; 10.1523/JNEUROSCI.0828-19.2019

Received: 3 April 2019
Revised: 22 July 2019
Accepted: 29 July 2019

This Early Release article has been peer-reviewed and accepted, but has not been through the composition and copyediting processes. The final version may differ slightly in style or formatting and will contain links to any extended data.

Alerts: Sign up at www.jneurosci.org/alerts to receive customized email alerts when the fully formatted version of this article is published.

Copyright © 2019 the authors

JNeurosci Accepted Manuscript

The origin of GnRH pulse generation: An integrative mathematical-experimental approach

Margaritis Voliotis[1,2,*,†] , Xiao Feng Li[3, †], Ross De Burgh[3,†], Geffen Lass[3], Stafford L. Lightman[4], Kevin T. O'Byrne[3*], Krasimira Tsaneva-Atanasova[1,2,*]

[1] Department of Mathematics and Living Systems Institute, College of Engineering, Mathematics and Physical Sciences, University of Exeter, Exeter, EX4 4QF, UK.

[2] EPSRC Centre for Predictive Modelling in Healthcare, University of Exeter, Exeter, EX4 4QJ, UK.

[3] Department of Women and Children's Health, School of Life Course Sciences, King's College London, London SE1 1UL, UK.

[4] Henry Wellcome Laboratory for Integrative Neuroscience and Endocrinology, University of Bristol, Bristol, BS1 3NY, UK.

[†] These authors contributed equally to this work

[*] For correspondence: M.Voliotis@exeter.ac.uk, K.Tsaneva-Atanasova@exeter.ac.uk

Number of pages: 16

Number of figures: 6

Number of extended data tables: 0

Number of extended data figures: 0

Abstract: 146 words

Introduction: 643 words

Discussion: 1028 words

The authors declare no confict of interest.

Acknowledgments: The authors gratefully acknowledge the financial support of the EPSRC via grant EP/N014391/1 (KTA and MV), MRC via grant MR/N022637/1 (KOB and SLL), and BBSRCH via grant BB/S001255/1 (KTA, KOB, MV, XFL).

JNeurosci Accepted Manuscript

Abstract

Fertility critically depends on the gonadotropin-releasing hormone (GnRH) pulse generator, a neural construct comprised of hypothalamic neurons co-expressing kisspeptin, neurokoinin-B and dynorphin. Here, using mathematical modelling and in-vivo optogenetics we reveal for the first time how this neural construct initiates and sustains the appropriate ultradian frequency essential for reproduction. Prompted by mathematical modelling, we show experimentally using female estrous mice that robust pulsatile release of luteinizing hormone, a proxy for GnRH, emerges abruptly as we increase the basal activity of the neuronal network using continuous low frequency optogenetic stimulation. Further increase in basal activity markedly increases pulse frequency and eventually leads to pulse termination. Additional model predictions that pulsatile dynamics emerge from non-linear positive and negative feedback interactions mediated through neurokinin-B and dynorphin signaling respectively are confirmed neuropharmacologically. Our results shed light on the long-elusive GnRH pulse generator offering new horizons for reproductive health and wellbeing.

Significance Statement

The gonadotropin-releasing hormone (GnRH) pulse generator controls the pulsatile secretion of the gonadotropic hormones LH and FSH and is critical for fertility. The hypothalamic arcuate kisspeptin neurons are thought to represent the GnRH pulse generator, since their oscillatory activity is coincident with LH pulses in the blood; a proxy for GnRH pulses. However, the mechanisms underlying GnRH pulse generation remain elusive. We developed a mathematical model of the kisspeptin neuronal network and confirmed its predictions experimentally, showing how LH secretion is frequency-modulated as we increase the basal activity of the arcuate kisspeptin neurons in-vivo using continuous optogenetic stimulation. Our model provides a quantitative framework for understanding the reproductive neuroendocrine system and opens new horizons for fertility regulation.

Introduction

The periodic release of gonadotropin-releasing hormone (GnRH) plays a central role in control of mammalian reproduction and is driven by hypothalamic neuronal networks (Herbison, 2016). The operation of these networks at a frequency appropriate for the species is critical for the generation of gonadotropin hormone signals (luteinizing hormone, LH; and follicle-stimulating hormone, FSH) by the pituitary gland, which stimulate the gonads and set in motion gametogenesis and ovulation. However, the origin of GnRH pulse generation and mechanisms underlying frequency control remain poorly understood.

Secretion of GnRH by GnRH neurons located in the hypothalamus into the pituitary portal circulation is controlled by upstream hypothalamic signals (Herbison, 2016). The neuropeptide kisspeptin has been identified as a key regulator of GnRH secretion as both humans and rodents with inactivating mutations in kisspeptin or its receptor fail to progress through puberty or show normal pulsatile LH secretion (de Roux et al., 2003; Seminara et al., 2003; Kaiser, 2015). Within the hypothalamus, two major kisspeptin producing neuronal populations are found in the arcuate nucleus (ARC) and in the preoptical area (Hrabovszky, 2014) or the anteroventral periventricular (AVPV)/rostral periventricular (PeN) continuum in rodents (Clarkson et al., 2009). Moreover, the invariable association between neuronal activity in the ARC and LH pulses across a range of species from rodents to primates (Plant and Zeleznik, 2014) has been suggestive that the ARC is the location of the GnRH pulse generator, and therefore the ARC kisspeptin neurons, also known as KNDy for co-expressing neurokinin B (NKB) and dynorphin (Dyn) alongside kisspeptin (Lehman et al., 2011), constitute the core of the GnRH pulse generator.

JNeurosci Accepted Manuscript

Although animal studies have shown that KNDy neurons are critical for the regulation of GnRH secretion, there has been relatively little understanding on the regulatory mechanisms involved in generating and sustaining pulsatile dynamics. Pharmacological modulators of kisspeptin, NKB and Dyn signaling have been extensively used to perturb the system and study the effect on the activity of a hypothalamic neuronal population (using ARC multiunit activity (MUA) volleys, an electrophysiological correlate of GnRH pulse generator activity, as a proxy) (Wilson et al., 1984), as well as on downstream GnRH/LH pulse dynamics (Kinsey-Jones et al., 2008; Navarro et al., 2009; Wakabayashi et al., 2010; Kinsey-Jones et al., 2011). For example, it has been shown that kisspeptin (Kp-10) administration does not affect MUA volleys in the ovariectomized rat (Kinsey-Jones et al., 2008), suggesting that kisspeptin is relaying the pulsatile signal to GnRH neurons rather than generating it. On the contrary, administration of NKB or Dyn modulates MUA volley frequency in the ovariectomized goat (Wakabayashi et al., 2010), suggesting a more active role for these neuropeptides in the generation of the pulses. Deciphering, however, the role of NKB has been problematic, and there exist conflicting data showing either an increase or decrease of LH levels in response to administration of a selective NKB receptor (TACR3) agonist (senktide) (Sandoval-Guzmán and E Rance, 2004; Navarro et al., 2009; Kinsey-Jones et al., 2011). Recently, a study combining optogenetics, with whole-cell electrophysiology and molecular pharmacology has shed light on the action of the neuropeptides NKB and Dyn in the KNDy network (Qiu et al., 2016), with the key mechanistic finding that NKB functions as an excitatory signal by depolarizing KNDy cells at the post-synaptic site, while co-released Dyn functions pre-synaptically to inhibit NKB release.

Taking into account the experimental findings described above, we develop a mathematical model of the ARC KNDy network. The model predicts that this neuronal population behaves as a relaxation oscillator, autonomously generating and sustaining pulsatile activity similar to the hypothalamic MUA volleys observed *in vivo* (Wilson et al., 1984; Kinsey-Jones et al., 2011). Further model analysis reveals that basal activity within the ARC KNDy population is a critical for GnRH/LH pulsatility. We test this predictions *in-vivo* using optogenetics and show that LH secretion dynamics are sentsitive to *continuous* stimulation of the ARC KNDy network.

Materials and methods

Animals

Breeding pairs of Kiss-Cre heterozygous transgenic mice (Yeo et al., 2016) were obtained from the Department of Physiology, Development and Neuroscience, University of Cambridge, UK. Litters from the breeding pairs were genotyped by polymerase chain reaction (PCR) analysis. Adult female mice (8-14 wk old; 25-30g) heterozygous for the Kiss-Cre transgene or wild-type C57BL/6 littermates, with normal pubertal development and estrous cyclicity, were used. Mice were housed under a 12:12 h light/dark cycle (lights on 0700 h) at 22 ± 2 °C and provided with food (standard maintenance diet; Special Dietary Services, Wittam, UK) and water ad libitum. All animal procedures performed were approved by the Animal Welfare and Ethical Review Body (AWERB) Committee at King's College London, and in accordance with the UK Home Office Regulations.

Surgical procedures

Surgical procedures for stereotaxic injection of AAV9-EF1-dflox-hChR2-(H134R)-mCherry-WPRE-hGH (4.35 x 1013 GC/ml; Penn Vector Core) to express channelrhodopsin (ChR2) in ARC kisspeptin neurons were performed under aseptic conditions with general anesthesia induced by ketamine (Vetalar, 100 mg/kg, i.p.; Pfizer, Sandwich, UK) and xylazine (Rompun, 10 mg/kg, i.p.; Bayer, Leverkusen, Germany). Kiss-Cre female mice (n = 9) or wide-type (n = 3) were secured in a David

JNeurosci Accepted Manuscript

Kopf Motorized stereotaxic frame and surgical procedures were performed using a Robot Stereotaxy system (Neurostar, Tubingen, Germany). A small hole was drilled into the skull at a location above the ARC. The stereotaxic injection coordinates used to target the ARC were obtained from the mouse brain atlas of Paxinos and Franklin (Paxinos and Franklin, 2004) (0.3 mm lateral, 1.2 mm posterior to bregma and at a depth of 6.0 mm). Using a 2-µL Hamilton micro-syringe (Esslab, Essex, UK) attached to the Robot Stereotaxy, 1 µl of the AAV-construct was injected unilaterally into the ARC at a rate of 100 nl/min. The needle was left in position for a further 5 min and then removed slowly over 1 min. A fiber optic cannula (200 µm, 0.39NA, 1.25mm ceramic ferrule; Thorlabs LTD, Ely, UK) was then inserted at the same co-ordinates as the injection site, but to a depth of 5.88 mm, so that the fiber optic cannula was situated immediately above the latter. Dental cement or a glue composite was then used to fix the cannula in place, and the skin incision closed with suture. A separate group of mice (n = 10) injected with the AAV construct, and fiber optic cannulae as described above, but additionally chronically implanted with an intra-cerebroventricular (icv) fluid cannulae (26 gauge; Plastics One, Roanoke, VA, USA) targeting the lateral ventricle (coordinates: 1.1 mm lateral, 1.0 mm posterior to bregma and at a depth of 3.0 mm), was used for the combined neuropharmacological and optogenetic studies. After surgery, mice were left for 4 weeks to achieve effective opsin expression. After a 1-wk recovery period, the mice were handles daily to acclimatize them to the tail-tip blood sampling procedure (Steyn et al., 2013).

Validation of AAV injection site

After completion of experiments, mice were anaesthetized with a lethal dose of ketamine and transcardially perfused with heparinized saline for 5 min, followed by 10 min of ice-cold 4% paraformaldehyde (PFA) in phosphate buffer (pH 7.4) for 15 min using a pump (Minipuls, Gilson, Villiers Le Bel, France). Brains were rapidly collected and postfixed sequentially at 4 °C in 15% sucrose in 4% PFA and in 30% sucrose in phosphate-buffered saline until they sank. Afterwards, brains were snap-frozen on dry ice and stored at -80 °C until processing. Brains were coronally sectioned (40-µm) using a cryostat (Bright Instrument Co., Luton, UK) and every third section was collected between -1.34 mm to -2.70 mm from the bregma. Sections were mounted on microscope slides, air-dried and cover slipped with ProLong Antifade mounting medium (Molecular Probes, Inc. OR, USA). The injection site was verified and evaluated using Axioskop 2 Plus microscope equipped with axiovision 4.7. One of 19 Kiss-Cre mice failed to show mCherry fluorescence in the ARC and was excluded from the analysis.

Experimental design, and blood samplings for LH measurement

Prior to optogenetic stimulation, the very tip of the mouse's tail was excised using a sterile scalpel for subsequent blood sample collection (Czieselsky et al., 2016). The chronically implanted fiber optic cannula was then attached via a ceramic mating sleeve to a multimode fiber optic rotary joint patch cables (Thorlabs), allowing freedom of movement of the animal, for delivery of blue light (473 nm wavelength) using a Grass SD9B stimulator controlled DPSS laser (Laserglow Technologies, Toronto, Canada). Laser intensity at the tip of the fiber optic patch cable was 5 mW. After 1 h acclimatization, blood samples (5µl) were collected every 5 min for 2.5 h. After 1 h controlled blood sampling, continuous optic stimulation (5-ms pulse width) was initiated at 0.5, 1 and 5 Hz for 90 min. Controls received no optic stimulation. Kiss-Cre mice received the stimulation protocols in random order. Wild-type received 5 Hz optic stimulation only.

For the neuropharmacological manipulation of Dyn or NKB signaling with or without simultaneous optogenetic stimulation the animals were appropriately prepared as described above, but in addition an icv injection cannula with extension tubing, preloaded with drug solution (nor-BNI or SB222200

JNeurosci Accepted Manuscript

dissolved in artificial cerebrospinal fluid), was inserted into the guide cannula immediately after connection of the fiber optic cannula. The tubing was extended outside the cage and connected to a 10 µl syringe (Hamilton) mounted in an automated Harvard pump (Harvard Apparatus, Holliston, MA, USA) to allow remote microinfusion without disturbing the mice during the experiment. Five min before optic stimulation, icv administration of drug treatment commenced as a bolus injection over 5 min, followed by a continuous infusion for the remainder of the experiment. In the absence of optic stimulation the same icv regimen was used. The blood samples were frozen at -80°C until assayed. LH was measured using an in-house ELISA similar to that described by Steyn *et al.* (Steyn et al., 2013). Mouse LH standard (AFP-5306A; NIDDK-NHPP) and primary antibody (polyclonal antibody, rabbit LH antiserum, AFP240580Rb; NIDDK-NHPP) were purchased from Harbour-UCLA, CA, USA, and secondary antibody (Donkey anti-rabbit IgG polyclonal antibody [Horseradish peroxidase]; NA934) was purchased from VWR International, UK. The ELISA validation was carried out according to the procedure of Steyn *et al.* (Steyn et al., 2013). which was derived from protocols defined by the International Union of Pure and Applied Chemistry. The linear detection range was determined by assessment of 9 serially diluted mLH standard replicates ranging from 0.00195 to 1ng/ml. To interpolate the LH concentration in whole blood samples, a nonlinear regression analysis was performed using serially diluted mLH standards of known concentration to create a standard curve with a detection range from 8.0-0.015 ng/ml. Extension of the standard curve by inclusion of a top standard of 1.0 ng/ml and extrapolation of unknowns after nonlinear regression analysis allowed a theoretical detection range of whole blood mLH (in a 1:25 dilution) of 0.187 to 25ng/mL. In our hand, the sensitivity of the ELISA is 7.5pg/ml. Accuracy, intra- and inter-assay variability were determined using mouse blood samples with known amounts of mLH included in each assay. We observed reliable detection of mLH at a final concentration of 0.0039 ng/ml. A linear regression across a standard curve ranging from 0.0075 to 1.0 ng/ml generated an R^2 value of 0.964. The intra-assay and inter-assay variations were 4.6% and 10.2%, respectively.

LH Pulses and Statistical Analysis

Detection of LH pulses was established by use of the Dynpeak algorithm (Vidal et al., 2012). The effect of optogenetic stimulation on parameters of LH secretion was calculated by comparing the mean number of LH pulse per hour, within the 90 min stimulation/drug delivery period with the 60 min pre-stimulation/drug delivery control period. For the non-stimulated control animals, the same timepoints were compared. The mean number of LH pulse per hour, within the 90 min stimulation period, or equivalent, was also compared between experimental groups. Statistical significance was tested using one-way ANOVA followed by Dunnett's test. $P < 0.05$ was considered statistically significant. Data are presented as the mean ± SEM.

Modelling the effect of NKB and Dyn receptor antagonists

To model the effect of SB22222, a selective NKB receptor (TACR3) antagonist, we modify the expression for the synaptic input, I, to read:

$$I = I_0 + p_v \frac{N^{n_4}}{N^{n_4} + E^{n_4} + K_N^{n_4}} \bar{v},$$

Similarly to model the effect of nor-BNI, a kappa-opioid receptor antagonist, we modify function f_N to read:

$$f_N(\bar{v}, \bar{D}) = k_{N,0} + k_N \frac{\bar{v}^{n_2}}{\bar{v}^{n_2} + K_{v,2}^{n_2}} \frac{K_D^{n_3} + E^{n_3}}{\bar{D}^{n_3} + E^{n_3} + K_D^{n_3}}.$$

In the equations above parameter E represents the antagonist concentration.

Model callibration

JNeurosci Accepted Manuscript

We used an Approximate Bayesian Computation (ABC) method based on sequential Monte Carlo (SMC) (Toni et al., 2009) to infer model parameters d_D, d_N, k_D, $k_{D,0}$, and $k_{N,0}$ from MUA recordings (figure 3A in (Kinsey-Jones et al., 2012)). In ABC SMC a population of parameter vectors or particles, θ, initially sampled form the prior distribution π_0, is propagated to the approximate target posterior distribution $\pi_T(\theta|\, d(x(t), x^*(t)) < \varepsilon_T)$, where $d(x(t), x^*(t))$ is a discrepnacy function comparing the simulated dataset $x^*(t)$ to the experimental data $x(t)$, and ε_T is the error tolerance level. Propagation is accomplished through a sequence of distributions $\pi_i, i = 1, \dots, T-1$, associated with a series of decreasing tolerance levels ε_i, hence making the transition to the target π_T more gradual and avoiding getting stuck in areas of low probability. We used the following discrepancy function to comparing simulated $(x^*(t))$ to experimental $(x(t))$ data:

$$d(x(t), x^*(t)) = \max\left(\frac{I\big(x(t)\big) - I(x^*(t))}{I(x(t))}, \frac{DC\big(x(t)\big) - DC(x^*(t))}{DC(x(t))}\right)$$

where $I(z(t))$ is the average time interval between pulses in trajectory $z(t)$ and $DC(z(t))$ is the average duty cycle in $z(t)$ (defined as the fraction of time the activity exceeds 50% of the max activity). In the data we used $I\big(x(t)\big) = 19.26 \pm 0.32$min and $DC\big(x(t)\big) = 0.181 \pm 0.04$. Simulated trajectories were generated by simulating the model to 6000min and discarding the first 1000min. To ensure gradual transition between populations we take $T = 4$ and $\varepsilon_i = 10^{2-i}$. The size of the particle population is set to 500. The following prior distributions were used: $\log_{10}(d_D) \sim Uniform(-3,3)$, $\log_{10}(d_N) \sim Uniform(-3,3)$, $\log_{10}(k_D) \sim Uniform(-3,3)$, $\log_{10}(k_{D,0}) \sim Uniform(-3,3)$, $\log_{10}(k_{N,0}) \sim Uniform(-3,3)$. All remaining parameters were fixed to values found in the literature (see Table 1). For each parameter an indepedndent $\log_{10}$-normal perturbation kernel with variance 0.05 was used.

Bifurcation analysis and numerical experiments

Bifurcation analysis of the model was performed using AUTO-07p (Doedel et al., 2007). The model was simulated in Matlab using function ode45 (explicit Runge-Kutta (4, 5) solver).

Results

A coarse-grained model of the ARC KNDy population

We propose a mathematical model (Figure 1A) to study the dynamics of the ARC KNDy population. The model describes the dynamics of the neuronal population using three variables: $\bar{D}$, representing the average concentration of Dyn secreted by the population; $\bar{N}$, representing the average concentration of NKB secreted by the population; and $\bar{v}$, representing the average firing activity of the population, measured in spikes/min. The dynamics of the model variables are governed by the following set of coupled ordinary differential equations (ODEs):

$$\frac{d\bar{D}}{dt} = f_D(\bar{v}) - d_D\bar{D}; \qquad [1]$$

$$\frac{d\bar{N}}{dt} = f_N(\bar{v}, \bar{D}) - d_N\bar{N}; \qquad [2]$$

$$\frac{d\bar{v}}{dt} = f_v(\bar{v}, \bar{N}) - d_v\bar{v}. \qquad [3]$$

Parameters d_D, $d_N$and d_v control the characteristic timescale of each variable. In particular, parameters d_D and d_N correspond to the rate at which Dyn and NKB are lost (e.g. due to diffusion or active

JNeurosci Accepted Manuscript

degradation), while d_v relates to the rate at which neuronal activity resets to its basal level. Functions f_D, f_N describe the secretion rate of Dyn and NKB, respectively, while function f_v encodes how the firing rate changes in response to the current levels of NKB and firing rate.

We employ the following sigmoidal (Hill) functions to describe regulatory relationships between the state variables. In particular, we set the secretion rate of Dyn and NKB to be:

$$f_D(\bar{v}) = k_{D,0} + k_D \frac{\bar{v}^{n_1}}{\bar{v}^{n_1} + K_{v,1}^{n_1}};$$

$$f_N(\bar{v}, \bar{D}) = k_{N,0} + k_N \frac{\bar{v}^{n_2}}{\bar{v}^{n_2} + K_{v,2}^{n_2}} \frac{K_D^{n_3}}{\bar{D}^{n_3} + K_D^{n_3}}.$$

In the equations above, both neuropeptides are constitutively secreted at rates $k_{D,0}$ and $k_{N,0}$, neuronal activity stimulates secretion of the two neuropeptides, and Dyn represses NKB secretion (Qiu et al., 2016). Since the rate of neuropeptide release is inherently limited by availability of cytoplasmic secretory vesicles at the presynaptic terminals (Han et al., 1999), we let secretion rates saturate at k_D and k_N, respectively. The effector levels at which saturation occurs are controlled via parameters $K_{v,1}$, $K_{v,2}$ and K_D. Furthermore, we set:

$$f_v(\bar{v}, \bar{N}) = v_0 \frac{1 - \exp(-I)}{1 + \exp(-I)};$$

$$I = I_0 + p_v \frac{N^{n_4}}{N^{n_4} + K_N^{n_4}} \bar{v},$$

where v_0 is the maximum rate at which the firing rate increases in response to synaptic inputs I. The stimulatory effect of NKB (which is secreted at the presynaptic terminal) is mediated via G protein-coupled receptor Tacr3 and is manifested as a short-term depolarization of the postsynaptic neuron (Qiu et al., 2016). In the equation above, we accommodate this effect by letting a synaptic weight that is a sigmoidal function of NKB multiply $\bar{v}$. Parameter K_N sets the level of NKB at which its effect is half-maximal, and parameter p_v controls the strength of the synaptic connections between KNDy neurons. Finally, parameter I_0 controls the basal neuronal activity in the population, which could stem from synaptic noise or external inputs. We find that for biophysically relevant parameter values (Table 1) the model predicts events of synchronized neuronal activity (Figure 1A), reminiscent of the activity measured from the arcuate nucleus of rodent models (Kinsey-Jones et al., 2011; Clarkson et al., 2017b), and supports the hypothesis that KNDy neurons in the ARC constitute the core of the GnRH pulse generator (Clarkson et al., 2017b).

Analysis of the model reveals the KNDy population functions as a relaxation oscillator.

Having shown that the model can reproduce sustained pulses of neuronal activity, we proceed to investigate the mechanisms driving the phenomenon. We first study the role of Dyn-mediated negative feedback using fast – slow analysis (Rinzel, 1985) of the coarse-grained model (Eqns. [1–3]). Model calibration suggests that Dyn operates at a slower time-scale than NKB (Table 1). This time-scale separation, also supported by receptor internalization data (Weems et al., 2018), allows us to study the dynamics of the fast subsystem, comprised of $\bar{N}$ and $\bar{v}$, as a function of the slow variable, $\bar{D}$, which is treated as a constant (bifurcation) parameter. Our analysis shows that for intermediate values of Dyn the fast subsystem can exist either in a high or a low activity state (Figure 1B). This bi-stable behavior, stemming from the non-linear positive feedback between neuronal activity and NKB secretion, leads to sustained oscillations of neuronal activity when combined with slow, Dyn-mediated, negative feedback. In engineering terms, the system behaves as a relaxation oscillator: where the bi-stable subsystem is successively excited (moved from low to high state) by external inputs or noise and silenced (moved from high to low state) as a result of negative feedback. We should note that a

JNeurosci Accepted Manuscript

relatively slow negative feedback is sufficient for sustaining oscillations, however, the combination of negative feedback with bi-stability is found in many biological oscillators most likely because it confers robustness (Pomerening et al., 2003).

Next, to demonstrate the role of basal neuronal activity within the KNDy network in the generation and modulation of oscillatory activity, we treat parameter I_0 as a bifurcation parameter. Our analysis shows that oscillatory behavior is supported within a critical range of I_0 values (see Figure 1C). As I_0 is increased from zero, high-amplitude, low-frequency pulses emerge via a Hopf bifurcation (Figure 1C; HB1 point). The frequency of pulses further increases with I_0, until oscillations disappear via a Hopf bifurcation (Figure 1C; HB2 point) and the system re-enters a silent (non-oscillatory) regime.

Continuous optogenetic stimulation of KNDy neurons alters the pattern of LH secretion *in vivo*.

To test the model prediction that basal excitation within the KNDy population contols LH pulsatility, we continuously stimulated the ARC KNDy population in Kiss-Cre mice (Adekunbi et al., 2018) using optogenetics and measured LH dynamics. ARC kisspeptin-expressing neurons were transduced with a Cre-dependent adeno-associated virus (AAV9-EF1-dflox-hChR2-(H134R)-mCherry-WPRE-hGH) to express ChR2 (Figure 2). AAV-injected, Kiss-Cre mice were implanted with a fiber optic cannula in the ARC and the effects on LH pulsatility of continuous stimulation at different frequencies was tested. After 1 h of controlled blood sampling, low-frequency optic stimulation, 5-ms pulses of blue light (473 nm) at 0.5, 1 or 5 Hz, was initiated and continuously delivered for 90 min. Control mice received no optic stimulation. During the course of the experiment, blood samples (5µl) were collected every 5 min (Adekunbi et al., 2018). To maximize the effect of optogenetic stimulation, estrous mice were used which display minimum intrinsic pulse generator activity (Czieselsky et al., 2016). Indeed, the majority of the control non-optically stimulated Kiss-Cre mice in estrus exhibited no LH pulse or intermittently 1 pulse during the 2.5 h sampling period (Figure 3A&G). Similarly, no LH pulses or occasionally 1 LH pulse was observed in the 60 min control period in the optically stimulated mice (Figure 3G; white bars). Continuous optic stimulation at 0.5 Hz failed to induce LH pulses (Figure 3B&G), while 1 Hz evoked regular LH pulses (Figure 3C&G), in line with our theoretical prediction of sudden qualitative changes in the dynamic behaviour of the system (Figre 1C). Stimulation at 5 Hz resulted in a further, statistically significant ($p < 0.05$), increase in LH pulse frequency (Figure 3D&G) further confirming that increasing the basal activity in the ARC KNDy neuronal population via low frequency continuous stimulation modulates LH pulsatile dyanmics. Further increasing the frequency of optic stimulation to 15Hz led to a reduction in LH pulses (Figure 3E&G), and at 20Hz the frequency of LH pulses under optic stimulation was indistinguishable from the control period (Figure 3F&G). Continuous optogenetic stimulation (5 Hz) of AAV-injected wild-type C57BL/6 estrous mice ($n = 3$) failed to induce LH pulses (data not shown).

Levels of Dyn and NKB signaling control the response of the system to optic stimulation.

The above theoretical and experimental results indicate a characteristic tipping-point behavior of the system, where a small increase in the basal activation levels is sufficient to trigger robust pulsatile dynamics (Strogatz, 2018). Our model predicts that such behavior emerges as a result of the non-linear positive and negative feedback interactions that are mediated through NKB and Dyn signaling respectively. Therefore to test the active role of NKB and Dyn signaling on pulse generation, we next combined optogenetic stimulation with neuropharmacological perturbations of the two pathways.

Disrupting Dyn signaling increases the sensitivity of the system to optic stimulation. Our model predicts that disruption of Dyn signaling should enable pulsatile dynamics over a wider range of optic stimulation frequencies (Figure 4A). Specifically, Figure 4A bottom panel depicts a two-parameter

JNeurosci Accepted Manuscript

bifurcation digram showing how the loci of HB1 and HB2 (see Figure 1C) change as we vary two parameters in the model, namely the basal activity (I_0) and antagonist concetration (E; see Materials and methods). Intuitively, such disruption will reduce the strength of negative feedback in the system and consequently lower optic stimulation frequencies would suffice to excite the bi-stable neuronal population and set the relaxation oscillator in motion. To test this prediction *in-vivo* we repeated the optogenetic stimulation protocol at 0.5Hz together with nor-binaltorphimine (nor-BNI), a selective kappa opioid receptor (KOR) antagonist, to block Dyn signaling. Although 0.5Hz had previously failed to induce LH pulses (Figure 4C&F), the addition of nor-BNI (bolus intra-cerebroventricular injection of 1.06 nmol over 5 min, followed by a continuous infusion of 1.28 nmol over 90 min) evokes a statistically significant increase in LH pulse frequency to approximately 1.6 pulses/hour (Figure 4E&F). Intra-cerebroventricular injection of nor-BNI alone had no effect on LH pulse frequency (Figure 4D&F).

Disrupting NKB signaling desensitizes the system to optic stimulation. Our model also predicts that disruption of NKB signaling should desensitize the system to external optic stimulation (see Figure 5A). Specifically, Figure 5A bottom panel depicts a two-parameter bifurcation digram showing how the loci of HB1 and HB2 (see Figure 1C) change as we vary two parameters in the model, namely the basal activity (I_0) and antagonist (E; see Materials and methods). NKB signaling is key for pulsatile behavior as it enables positive feedback interactions within the population and therefore promotes bi-stability. Hence disrupting NKB signaling ought to decrease the propensity of the system to get excited into the pulsatile regime by external stimulation. To test this prediction *in-vivo* we repeated the optogenetic stimulation protocol at the highest frequency (5Hz), and used SB222200, a selective TACR3 antagonist, to block NKB signaling. Although 5Hz had previously induced a high frequency LH response (Figure 4C&F), we observe that antagonist addition (bolus intra-cerebroventricular injection of 6 nmol over 5 min, followed by a continuous infusion of 9 nmol over 90 min) completely blocked the increased LH pulse frequency (Figure 5E&F). Intra-cerebroventricular injection of SB222200 alone had no effect on LH pulse frequency (Figure 5D&F).

Discussion

We developed and studied a mathematical model of the KNDy neural population in the ARC, a population proposed to comprise the core of the GnRH pulse generator (Clarkson et al., 2017a; Fergani and Navarro, 2017). Our model demonstrates that the KNDy population can indeed produce and sustain pulsatile dynamics working as a relaxation oscillator. On the one hand, auto-stimulation via NKB signaling allows the population to behave as a bi-stable switch, firing either at a high or low rate. Moreover, basal neuronal activity and negative feedback through Dyn signaling allow the population to switch between the two activity states in a regular manner, giving rise to pulses of neuronal activity. Using global sensitivity analysis, we found that this mechanism of pulse generation is robust to parameter perturbations (Figure 6). In fact, co-variation of parameters governing, for example, the magnitude of basal activity, and the maximum secretion rates of NKB and Dyn is a more effective way of modulating the systems' oscillatory behavior (amplitude and frequency). This multi-channel mode of efficient regulation is perhaps not surprising given the system's crucial function, and hints that steroid feedback modulating the dynamics of the pulse generator over the reproductive cycle in female mammals is mediated through multiple, possibly interlinked, pathways.

Our mathematical model presumes that KNDy neurons comprise the core mechanism behind GnRH pulse generation. However, there is ongoing debate over the precise definition of the GnRH pulse generator, and in particular whether pulse generation is intrinsic to the KNDy population or the donwstream GnRH neurons. The latter hypothesis is supported by data showing that continuous kisspeptin infusion can increase LH pulse frequency in women with hypothalamic amenorrhoea

JNeurosci Accepted Manuscript

(Jayasena et al., 2014); healthy men (George et al., 2011); patients with inactivating mutations in the NKB signalling pathway (Young et al., 2013); and in sheep in the presence of NKB antagonism (Clarke et al., 2018). These data do not exclude the KNDy hypothesesis nor directly contradict it, as continuous kisspeptin stimulation could be allowing GnRH neurons to respond to residual episodic KNDy activity, however they do highlight the possibility of multiple distinct mechanisms driving LH pulsatility (Lehnert and Khadra, 2019; Lippincott et al., 2019).

Following model predictions, we explored the effect of continuous optogenetic activation of the KNDy population on LH pulse dynamics, a proxy for GnRH pulse dynamics. Analysis of the model highlights that the KNDy population undergoes sudden qualitative changes in its dynamic behaviour as the basal activity of the population is modulated. In particular, as the basal activity level is increased the system transitions from a silent into a pulsatile mode, while higher levels of basal activity inhibit pulses and reinstate the quiescent state. Importantly, these sudden transitions are a rudimetrary characteristic of the mechanimsms underlying pulse generation, and hence should be experimentaly verifiable. We tested model predictions *in-vivo* using optogenetics (Campos and Herbison, 2014; Han et al., 2015b; Clarkson et al., 2017a), and showed that we are able to induce LH pulses in estrous mice by selectively exciting KNDy neurons in a continuous fashion between 1Hz and 5Hz. In-vitro arcuate kisspeptin neurons transfected with ChR2 responded with remarkable fidelity (>97%) to optic stimulation in the range 1-20Hz (Han et al., 2015a), eliciting a single action potential for each pulse of light they receive. This highlights the sudden emergenece of pulsatile dynamics as we increase optic stimulation form 0.5Hz to 1Hz, in par with the *qualitative* picture predicted by the model. It is also interesting to note that the optic stimulation frequencies for which we start to see an effect on LH pulsatility match the spontaneous activity measured from KNDy neurones in brain slices from intact (~1Hz), castrated (~5Hz) and castrated adult male mice treated with estradiol *in-vivo* (~1Hz) (Ruka et al., 2016). Stimulating at 15Hz elicited LH pulses but at a decreased frequency compared to 5Hz stimulation. This apparent slowing down of the pulse generator as the basal activity is increased could reflect fatigue of kisspeptin and/or GnRH secretion at higher stimulation frequencies or even non-linear dyanmics in the processing of GnRH singals by the pitutitary (Pratap et al., 2017), and stresses the need for direct in-vivo measurements of KNDy activity to probe in greater detail the dynamic mechanisms behind pulse generation and shed light on the multiple pulse generator hypothesis.

It is important to note that the model has informed the design of the experiments by suggesting the use of low-frequency optic stimulation for the first time in investigating LH pulse generation and in contrast to previous studies (Campos and Herbison, 2014; Han et al., 2015b; Clarkson et al., 2017a). Our results suggest that inhibitory or excitatory synaptic signaling within the KNDy neural population have a drastic effect on GnRH/LH pulse dynamics. We speculate that this enables KNDy neurons to integrate and transmit information regarding the overall state of the organism that is relevant for reproduction: for example, information on the emotional state and stress level through synaptic connections originating at the level of the amygdala (Lin et al., 2010), a key limbic brain structure; or information regarding the nutritional state of the organism through connections from Agouti-related peptide (AgRP)-expressing neurons in the hypothalamus (Padilla et al., 2017).

Last but not least, the model predicted that the systems' pulsatile behavior emerges as a result of the non-linear positive and negative feedback interactions that are mediated through NKB and Dyn signaling respectively. Using experimental protocol suggested by model analysis we showed that the response of the system to external optic stimulation indeed follows our NKB and Dyn signaling predictions. Our results highlight the need for a quantitative understanding of how the sex-steroid milieu affects the NKB and Dyn signaling pathways in the KNDy population. Such an understanding will lead to more accurate interpretation of results from *in-vivo* neuropharmacological perturbation experiments in various animal models and will shed light on the mechanisms underlying the regulation

JNeurosci Accepted Manuscript

of pulsatile LH secretion in various natural settings such as lactational amenorrhoea or pharmaceutic interventions including the hormone contraceptive pill. We envision that as hormonal measurement techniques advance (Liang et al., 2019), enabling accurate, real-time readouts from individuals at low cost, such predictive mathematical models would be a valuable tool for understanding of reproductive pathophysiology.

References

Adekunbi D, Li X, Lass G, Shetty K, Adegoke O, Yeo S, Colledge W, Lightman S, O'Byrne K (2018) Kisspeptin neurones in the posterodorsal medial amygdala modulate sexual partner preference and anxiety in male mice. Journal of neuroendocrinology 30:e12572.

Campos P, Herbison AE (2014) Optogenetic activation of GnRH neurons reveals minimal requirements for pulsatile luteinizing hormone secretion. Proceedings of the National Academy of Sciences 111:18387-18392.

Clarke IJ, Li Q, Henry BA, Millar RP (2018) Continuous Kisspeptin Restores Luteinizing Hormone Pulsatility Following Cessation by a Neurokinin B Antagonist in Female Sheep. Endocrinology 159:639-646.

Clarkson J, Danglemont de Tassigny X, Colledge WH, Caraty A, Herbison AE (2009) Distribution of Kisspeptin Neurones in the Adult Female Mouse Brain. Journal of Neuroendocrinology 21:673-682.

Clarkson J, Han SY, Piet R, McLennan T, Kane GM, Ng J, Porteous RW, Kim JS, Colledge WH, Iremonger KJ, Herbison AE (2017a) Definition of the hypothalamic GnRH pulse generator in mice. Proceedings of the National Academy of Sciences 114:E10216-E10223.

Clarkson J, Han SY, Piet R, McLennan T, Kane GM, Ng J, Porteous RW, Kim JS, Colledge WH, Iremonger KJ, Herbison AE (2017b) Definition of the hypothalamic GnRH pulse generator in mice. Proc Natl Acad Sci U S A 114:E10216-E10223.

Czieselsky K, Prescott M, Porteous R, Campos P, Clarkson J, Steyn FJ, Campbell RE, Herbison AE (2016) Pulse and surge profiles of luteinizing hormone secretion in the mouse. Endocrinology 157:4794-4802.

de Croft S, Piet R, Mayer C, Mai O, Boehm U, Herbison AE (2012) Spontaneous kisspeptin neuron firing in the adult mouse reveals marked sex and brain region differences but no support for a direct role in negative feedback. Endocrinology 153:5384-5393.

de Roux N, Genin E, Carel JC, Matsuda F, Chaussain JL, Milgrom E (2003) Hypogonadotropic hypogonadism due to loss of function of the KiSS1-derived peptide receptor GPR54. Proceedings of the National Academy of Sciences 100:10972-10976.

Doedel EJ, Fairgrieve TF, Sandstede B, Champneys AR, Kuznetsov YA, Wang X (2007) AUTO-07P: Continuation and bifurcation software for ordinary differential equations. In.

Dutton A, Dyball RE (1979) Phasic firing enhances vasopressin release from the rat neurohypophysis. J Physiol 290:433-440.

Fergani C, Navarro VM (2017) Expanding the role of tachykinins in the neuroendocrine control of reproduction. Reproduction 153:R1-R14.

George JT, Veldhuis JD, Roseweir AK, Newton CL, Faccenda E, Millar RP, Anderson RA (2011) Kisspeptin-10 is a potent stimulator of LH and increases pulse frequency in men. J Clin Endocrinol Metab 96:E1228-1236.

Han SY, McLennan T, Czieselsky K, Herbison AE (2015a) Selective optogenetic activation of arcuate kisspeptin neurons generates pulsatile luteinizing hormone secretion. Proc Natl Acad Sci U S A 112:13109-13114.

JNeurosci Accepted Manuscript

455 Han SY, McLennan T, Czieselsky K, Herbison AE (2015b) Selective optogenetic activation of arcuate
456 kisspeptin neurons generates pulsatile luteinizing hormone secretion. Proceedings of the
457 National Academy of Sciences 112:13109-13114.
458 Han W, Ng Y-K, Axelrod D, Levitan ES (1999) Neuropeptide release by efficient recruitment of
459 diffusing cytoplasmic secretory vesicles. Proceedings of the National Academy of Sciences
460 96:14577-14582.
461 Herbison AE (2016) Control of puberty onset and fertility by gonadotropin-releasing hormone neurons.
462 Nature Reviews Endocrinology 12:452-466.
463 Hrabovszky E (2014) Neuroanatomy of the Human Hypothalamic Kisspeptin System.
464 Neuroendocrinology 99:33-48.
465 Jayasena CN, Abbara A, Veldhuis JD, Comninos AN, Ratnasabapathy R, De Silva A, Nijher GM,
466 Ganiyu-Dada Z, Mehta A, Todd C, Ghatei MA, Bloom SR, Dhillo WS (2014) Increasing LH
467 pulsatility in women with hypothalamic amenorrhoea using intravenous infusion of Kisspeptin-
468 54. J Clin Endocrinol Metab 99:E953-961.
469 Kaiser UB (2015) Understanding reproductive endocrine disorders. Nature Reviews Endocrinology
470 11:640-641.
471 Kinsey-Jones JS, Li XF, Luckman SM, O'Byrne KT (2008) Effects of Kisspeptin-10 on the
472 Electrophysiological Manifestation of Gonadotropin-Releasing Hormone Pulse Generator
473 Activity in the Female Rat. Endocrinology 149:1004-1008.
474 Kinsey-Jones JS, Grachev P, Li XF, Lin YS, Milligan SR, Lightman SL, O'Byrne KT (2011) The
475 Inhibitory Effects of Neurokinin B on GnRH Pulse Generator Frequency in the Female Rat.
476 Endocrinology 153:307-315.
477 Kinsey-Jones JS, Grachev P, Li XF, Lin YS, Milligan SR, Lightman SL, O'Byrne KT (2012) The
478 inhibitory effects of neurokinin B on GnRH pulse generator frequency in the female rat.
479 Endocrinology 153:307-315.
480 Lehman MN, Coolen LM, Goodman RL (2011) Minireview: Kisspeptin/Neurokinin B/Dynorphin
481 (KNDy) Cells of the Arcuate Nucleus: A Central Node in the Control of Gonadotropin-
482 Releasing Hormone Secretion. Endocrinology.
483 Lehnert J, Khadra A (2019) How Pulsatile Kisspeptin Stimulation and GnRH Autocrine Feedback Can
484 Drive GnRH Secretion: A Modeling Investigation. Endocrinology 160:1289-1306.
485 Liang S, Kinghorn AB, Voliotis M, Prague JK, Veldhuis JD, Tsaneva-Atanasova K, McArdle CA, Li
486 RHW, Cass AEG, Dhillo WS, Tanner JA (2019) Measuring luteinising hormone pulsatility with
487 a robotic aptamer-enabled electrochemical reader. Nat Commun 10:852.
488 Lin Y, Li X, Lupi M, Kinsey-Jones JS, Shao B, Lightman SL, O'Byrne KT (2010) The role of the
489 medial and central amygdala in stress-induced suppression of pulsatile LH secretion in female
490 rats. Endocrinology 152:545-555.
491 Lippincott MF, Leon S, Chan YM, Fergani C, Talbi R, Farooqi IS, Jones CM, Arlt W, Stewart SE,
492 Cole TR, Terasawa E, Hall JE, Shaw ND, Navarro VM, Seminara SB (2019) Hypothalamic
493 Reproductive Endocrine Pulse Generator Activity Independent of Neurokinin B and Dynorphin
494 Signaling. J Clin Endocrinol Metab.
495 Marino S, Hogue IB, Ray CJ, Kirschner DE (2008) A methodology for performing global uncertainty
496 and sensitivity analysis in systems biology. J Theor Biol 254:178-196.
497 Navarro VM, Gottsch ML, Chavkin C, Okamura H, Clifton DK, Steiner RA (2009) Regulation of
498 Gonadotropin-Releasing Hormone Secretion by Kisspeptin/Dynorphin/Neurokinin B Neurons
499 in the Arcuate Nucleus of the Mouse. The Journal of Neuroscience 29:11859-11866.
500 Padilla SL, Qiu J, Nestor CC, Zhang C, Smith AW, Whiddon BB, Rønnekleiv OK, Kelly MJ, Palmiter
501 RD (2017) AgRP to Kiss1 neuron signaling links nutritional state and fertility. Proceedings of
502 the National Academy of Sciences:201621065.

JNeurosci Accepted Manuscript

503 Paxinos G, Franklin K (2004) The mouse brain in stereotaxic coordinates Amsterdam. In: Boston, MA:
504 Elsevier Academic Press.
505 Plant TM, Zeleznik AJ (2014) Knobil and Neill's physiology of reproduction: Academic Press.
506 Pomerening JR, Sontag ED, Ferrell JE (2003) Building a cell cycle oscillator: hysteresis and bistability
507 in the activation of Cdc2. Nature Cell Biology 5:346-351.
508 Pratap A, Garner KL, Voliotis M, Tsaneva-Atanasova K, McArdle CA (2017) Mathematical modeling
509 of gonadotropin-releasing hormone signaling. Mol Cell Endocrinol 449:42-55.
510 Qiu J, Nestor CC, Zhang C, Padilla SL, Palmiter RD, Kelly MJ, Ronnekleiv OK (2016) High-
511 frequency stimulation-induced peptide release synchronizes arcuate kisspeptin neurons and
512 excites GnRH neurons. Elife 5:e16246-e16246.
513 Rinzel J (1985) Bursting oscillations in an excitable membrane model. In: Ordinary and partial
514 differential equations, pp 304-316: Springer.
515 Ruka KA, Burger LL, Moenter SM (2016) Both Estrogen and Androgen Modify the Response to
516 Activation of Neurokinin-3 and kappa-Opioid Receptors in Arcuate Kisspeptin Neurons From
517 Male Mice. Endocrinology 157:752-763.
518 Sandoval-Guzmán T, E Rance N (2004) Central injection of senktide, an NK3 receptor agonist, or
519 neuropeptide Y inhibits LH secretion and induces different patterns of Fos expression in the rat
520 hypothalamus. Brain research 1026:307-312.
521 Seabrook GR, Bowery BJ, Hill RG (1995) Pharmacology of tachykinin receptors on neurones in the
522 ventral tegmental area of rat brain slices. Eur J Pharmacol 273:113-119.
523 Seminara SB, Messager S, Chatzidaki EE, Thresher RR, Acierno Jr JS, Shagoury JK, Bo-Abbas Y,
524 Kuohung W, Schwinof KM, Hendrick AG, Zahn D, Dixon J, Kaiser UB, Slaugenhaupt SA,
525 Gusella JF, O'Rahilly S, Carlton MBL, Crowley Jr WF, Aparicio SAJR, Colledge WH (2003)
526 The GPR54Gene as a Regulator of Puberty. New England Journal of Medicine 349:1614-1627.
527 Steyn FJ, Wan Y, Clarkson J, Veldhuis JD, Herbison A, Chen C (2013) Development of a
528 methodology for and assessment of pulsatile luteinizing hormone secretion in juvenile and adult
529 male mice. Endocrinology 154:4939-4945.
530 Strogatz SH (2018) Nonlinear dynamics and chaos: with applications to physics, biology, chemistry,
531 and engineering: CRC Press.
532 Toni T, Welch D, Strelkowa N, Ipsen A, Stumpf MP (2009) Approximate Bayesian computation
533 scheme for parameter inference and model selection in dynamical systems. J R Soc Interface
534 6:187-202.
535 Vidal A, Zhang Q, Médigue C, Fabre S, Clément F (2012) DynPeak: An algorithm for pulse detection
536 and frequency analysis in hormonal time series. PLoS One 7:e39001.
537 Wakabayashi Y, Nakada T, Murata K, Ohkura S, Mogi K, Navarro VM, Clifton DK, Mori Y,
538 Tsukamura H, Maeda K-I, Steiner RA, Okamura H (2010) Neurokinin B and Dynorphin A in
539 Kisspeptin Neurons of the Arcuate Nucleus Participate in Generation of Periodic Oscillation of
540 Neural Activity Driving Pulsatile Gonadotropin-Releasing Hormone Secretion in the Goat. The
541 Journal of Neuroscience 30:3124-3132.
542 Weems PW, Coolen LM, Hileman SM, Hardy S, McCosh RB, Goodman RL, Lehman MN (2018)
543 Evidence That Dynorphin Acts Upon KNDy and GnRH Neurons During GnRH Pulse
544 Termination in the Ewe. Endocrinology 159:3187-3199.
545 Wilson RC, Kesner JS, Kaufman J-M, Uemura T, Akema T, Knobil E (1984) Central
546 electrophysiologic correlates of pulsatile luteinizing hormone secretion in the rhesus monkey.
547 Neuroendocrinology 39:256-260.
548 Yasuda K, Raynor K, Kong H, Breder CD, Takeda J, Reisine T, Bell GI (1993) Cloning and functional
549 comparison of kappa and delta opioid receptors from mouse brain. Proc Natl Acad Sci U S A
550 90:6736-6740.

JNeurosci Accepted Manuscript

551 Yeo SH, Kyle V, Morris P, Jackman S, Sinnett-Smith L, Schacker M, Chen C, Colledge W (2016)
552 Visualisation of Kiss1 Neurone Distribution Using a Kiss1-CRE Transgenic Mouse. Journal of
553 neuroendocrinology 28.
554 Young J, George JT, Tello JA, Francou B, Bouligand J, Guiochon-Mantel A, Brailly-Tabard S,
555 Anderson RA, Millar RP (2013) Kisspeptin restores pulsatile LH secretion in patients with
556 neurokinin B signaling deficiencies: physiological, pathophysiological and therapeutic
557 implications. Neuroendocrinology 97:193-202.
558

JNeurosci Accepted Manuscript

Figure 1: **A coarse-grained model gives mechanistic insight into the pulsatile behavior of the ARC KNDy population.** (A) We developed a mean-field model of the neuronal population comprising three dynamical variables: $\overline{D}$, representing the average concentration of Dyn secreted; $\overline{N}$, representing the concentration of NKB secreted; and $\bar{v}$, representing the average firing activity of the neuronal population. The model predicts that the system behaves as a relaxation oscillator owning to NKB induced bistability and Dyn-mediated negative feedback. (B) Disrupting Dyn negative feedback obliterates the oscillatory behaviour of the system. For intermediate levels of externally provided Dyn, the system exhibits two stable equilibria (upper and lower solid lines) and an unstable one (dashed red line). At the edges of the bistable regime equilibria are lost through a saddle-node bifurcation (SD points). The bistability gives rise to hysteresis as the value of Dyn is varied externally (grey arrows). (C) The model predicts how basal neuronal activity affects the system's dynamics and pulse frequency. As basal activity is increased from zero, high-amplitude, low-frequency pulses emerge after some critical value (HB1 point; Hopf bifurcation). The frequency of pulses continues to increase with basal activity until oscillations disappear (HB2 point; Hopf bifurcation) and the system enters a mono-stable regime (black solid line). The solid red line denotes the amplitude of the pulses. Parameter values used in the bifurcation analysis are given in Table 1.

Figure 2: **Expression of arcuate nucleus (ARC) kisspeptin neurones with ChR2-mCherry in Kiss-CRE mice.** Coronal section showing red mCherry fluorescence positive neurones in the ARC which indicates ChR2 receptor expressing kisspeptin neurones, following unilateral injection of AAV9.EF1.dflox.hChR2(H134R)-mCherry.WPRE.hGH into the ARC of Kiss-Cre mice. The blue arrow shows the precise location of fiber optic for stimulation. Note the absence of mCherry fluorescence in the other side of ARC. 3V, third ventricle.

Figure 3: **Optic stimulation of ARC kisspeptin neurons triggers LH pulses in estrous Kiss-Cre mice**. (A-D) Representative examples showing LH secretion in response to no stimulation (grey bar) as control (A), or continuous blue light (473 nm, 5-ms pulse width, black bar) activation of kisspeptin neurons at 0.5 Hz (B), 1 Hz (C), 5 Hz (D), 15Hz (E), and 20Hz (F). Pulses detected by the DynePeak algorithm are indicated with an asterisk. (G) Summary showing for each group mean ± SEM LH pulse frequency over the 60min control period (white bars) and over the subsequent stimulation period (black bars). †P < 0.05 vs pre-stimulation; #P < 0.05 vs stimulation at higher frequency. n = 4-9 per group.

Figure 4: **Disrupting Dyn signaling increases the sensitivity of the system to optic stimulation**. (A) The model predicts that reducing the strength of negative feedback by partially blocking Dyn signaling should enable pulsatile dynamics over a wider range of optic stimulation frequencies as shown by the two-parameter bifurcation diagram depicting the region in the parameters (antagonist and basal activity) coloured in blue and defined by the loci of HB1 and HB2 (left and right curves respectively) that expands as antagonist is increased). Model parameter values are given in Table 1. (B-F) Nor-BNI, a Dyn receptor (kappa-opioid) antagonist, was used to block Dyn signaling *in-vivo*. Representative examples showing LH secretion in response to no treatment (grey bar) as control (B), continuous blue light (473 nm, 5-ms pulse width, black bar) activation of kisspeptin neurons at 0.5 Hz (C), nor-BNI treatment (bolus intra-cerebroventricular injection of 1.06 nmol in 1.25µl over 5 min, followed by a continuous infusion of 1.28 nmol in 1.5µl over 90 min (D) or combined nor-BNI treatment and optic stimulation at 0.5Hz (E). Pulses detected by the DynePeak algorithm are indicated with an asterisk. (F) Summary plot showing for each group mean±SEM LH pulse frequency over the pre-treatment (white bars) and treatment period (black bars). †P < 0.05 vs pre-treatment; $^{\#}$P < 0.05 vs only optic stimulation treatment. n = 4-6 per group.

Figure 5: **Disrupting NKB signaling desensitize the system to optic stimulation**. (A) The model predicts that weakening bi-stability by blocking NKB signaling should restrict the range of optic stimulation frequencies that trigger pulsatility as shown by the two-parameter bifurcation diagram depicting the region in the parameters (antagonist and basal activity) coloured in blue and defined by the loci of HB1 and HB2 that collide associated with shrinking of the blue region as antagonist is increased. Model parameter values are given in Table 1. (B-F) SB222200 (SB), an NKB receptor (TACR3) antagonist, was used to block NKB signaling *in-vivo*. Representative examples showing LH secretion in response to no treatment (grey bar) as control (B), continuous blue light (473 nm, 5-ms pulse width, black bar) activation of kisspeptin neurons at 5 Hz (C), SB222200 treatment (bolus intra-cerebroventricular injection of 6 nmol in 1.25µl over 5 min, followed by a continuous infusion of 9 nmol in 1.5µl over 90 min) (D) or combined SB222200 treatment and optic stimulation at 0.5Hz (E). Pulses detected by the DynePeak algorithm are indicated with an asterisk. (F) Summary plot showing for each group mean±SEM LH pulse frequency over the pre-treatment (white bars) and treatment period (black bars). †P < 0.05 vs pre-treatment. n = 4-6 per group.

Figure 6: **Global sensitivity analysis of the KNDy model.** Global sensitivity analysis of the model considering maximum response amplitude, amplitude of oscillations, and period of oscillations. First order (A) and total-order (B) sensitivity indices are shown for parameters k_D(maximum rate of Dyn secretion), k_N (maximum rate of NKB secretion) and I_0 (basal synaptic inputs). First order sensitivity indices indicate the proportion of variance of a response feature that is explained by variation in a parameter, keeping other parameters fixed. First order sensitivity indices, therefore, quantify the effect that single parameter perturbations have on the dynamics of the system. Total order sensitivity indices, on the other hand,

JNeurosci Accepted Manuscript

indicate the proportion of variance in a response feature that is explained by variation in a parameter, while allowing variation in another parameters as well. Therefore, the total order sensitivity index of a parameter is a proxy for the effect this parameters has on the dynamics of the systems in combination with other parameters. Global sensitivity analysis was performed in Matlab using eFast (Marino et al., 2008). The following parameter distributions were used: $\log_{10}(I_0) \sim Uniform(-1,1)$, $\log_{10}(k_D) \sim Uniform(-1,3)$, and $\log_{10}(k_N) \sim Uniform(-1,3)$. All other model parameters were fixed (see Table 1). The model was initialised at state $(\bar{D}, \bar{N}, \bar{v}) = (0,0,0)$ and run to 6000min. Response features (i.e., maximum response amplitude, amplitude of oscillations and the period of oscillation) were calculated from the response trajectory after discarding the first 1000 min.

No	Parameter	Description	Value	Ref.
1	d_D	Dyn degradation rate	0.25 min^{-1} [0.05, 0.3] min^{-1}	inferred
2	d_N	NKB degradation rate	1 min^{-1} [0.3, 109.3] min^{-1}	inferred
3	d_v	Firing rate reset rate	10 min^{-1}	(Qiu et al., 2016)
4	k_D	Maximum Dyn secretion rate	4.5 nM min^{-1} [2.76, 38.4] nM min^{-1}	inferred
5	k_N	Maximum NKB secretion rate	320 nM min^{-1}	(Ruka et al., 2016)
6	$k_{D,0}$	Basal Dyn secretion rate	0.175 nM min^{-1} [10^{-3}, 1.88] nM min^{-1}	inferred
7	$k_{N,0}$	Basal NKB secretion rate	0 nM min^{-1} [10^{-3}, 0.44] nM min^{-1}	inferred
8	p_v	Effective strength of synaptic input	1 min	fixed
9	v_0	Maximum rate of neuronal activity increase	30000 spikes min^{-2}	(Qiu et al., 2016)
10	K_D	Dyn IC_{50}	0.3 nM	(Yasuda et al., 1993)
11	K_N	NKB EC_{50}	32 nM	(Seabrook et al., 1995)
12	$K_{v,1}$	Firing rate for half-maximal Dyn secretion	1200 spikes min^{-1}	(Dutton and Dyball, 1979)
13	$K_{v,2}$	Firing rate for half-maximal NKB secretion	1200 spikes min^{-1}	(Dutton and Dyball, 1979)
14	I_0	Basal activity	0.2 (corresponding to 5 spikes sec^{-1})	(de Croft et al., 2012; Ruka et al., 2016)
15	n_1, n_2, n_3, n_4	Hill coeffcients	2 (dimensionless)	fixed

Table 1: **Model parameter values.** Parameters values were either found in the literature or inferred from MUA rat data (Kinsey-Jones, 2012; Figure 3A). Here, we report the 99% equal tail posterior density interval for the marginal distribution of each inferred parameter. Along these intervals we report specific parameter values used for the bifurcation analysis and numerical evaluation of the model.

JNeurosci Accepted Manuscript

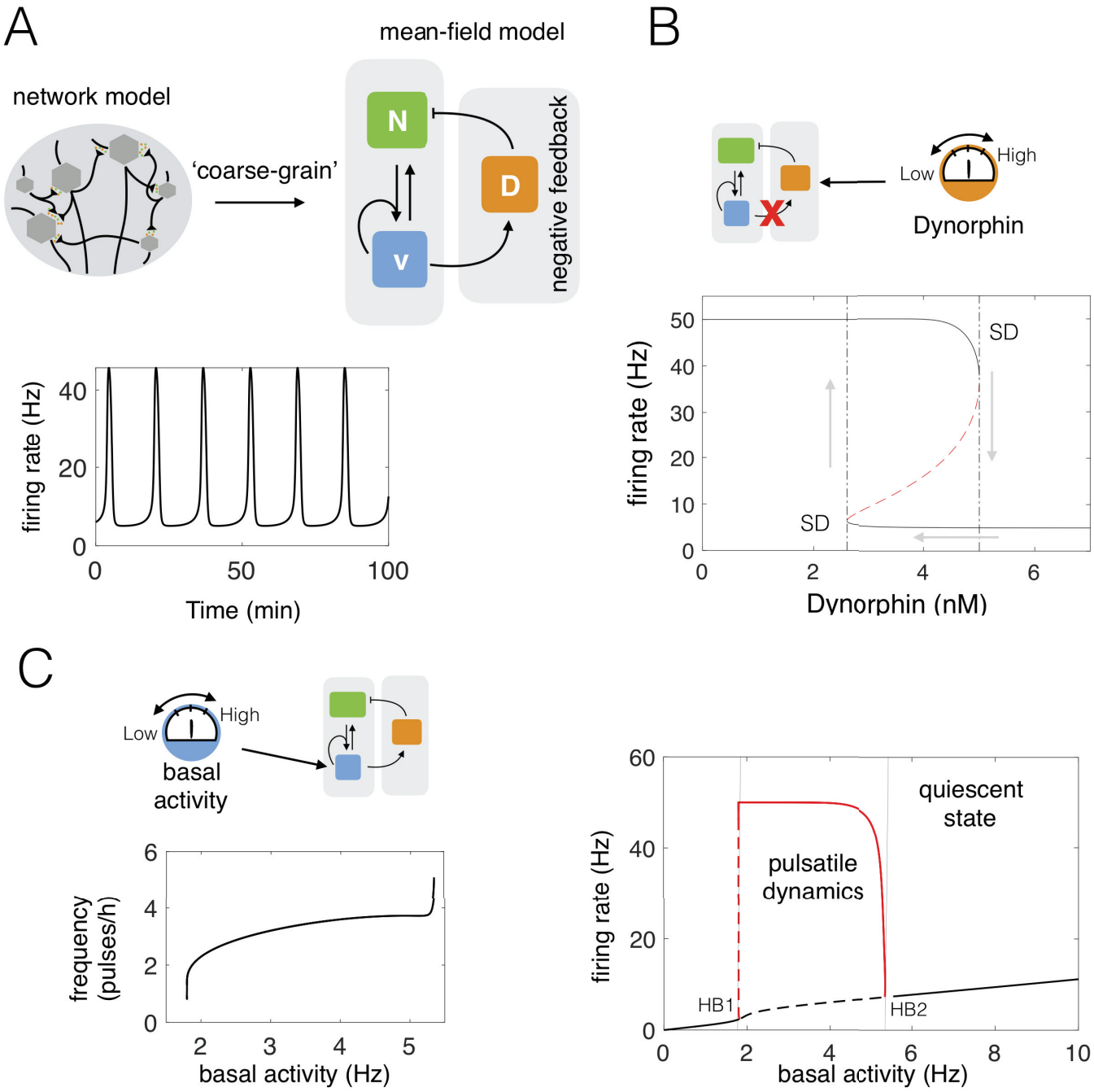

JNeurosci Accepted Manuscript

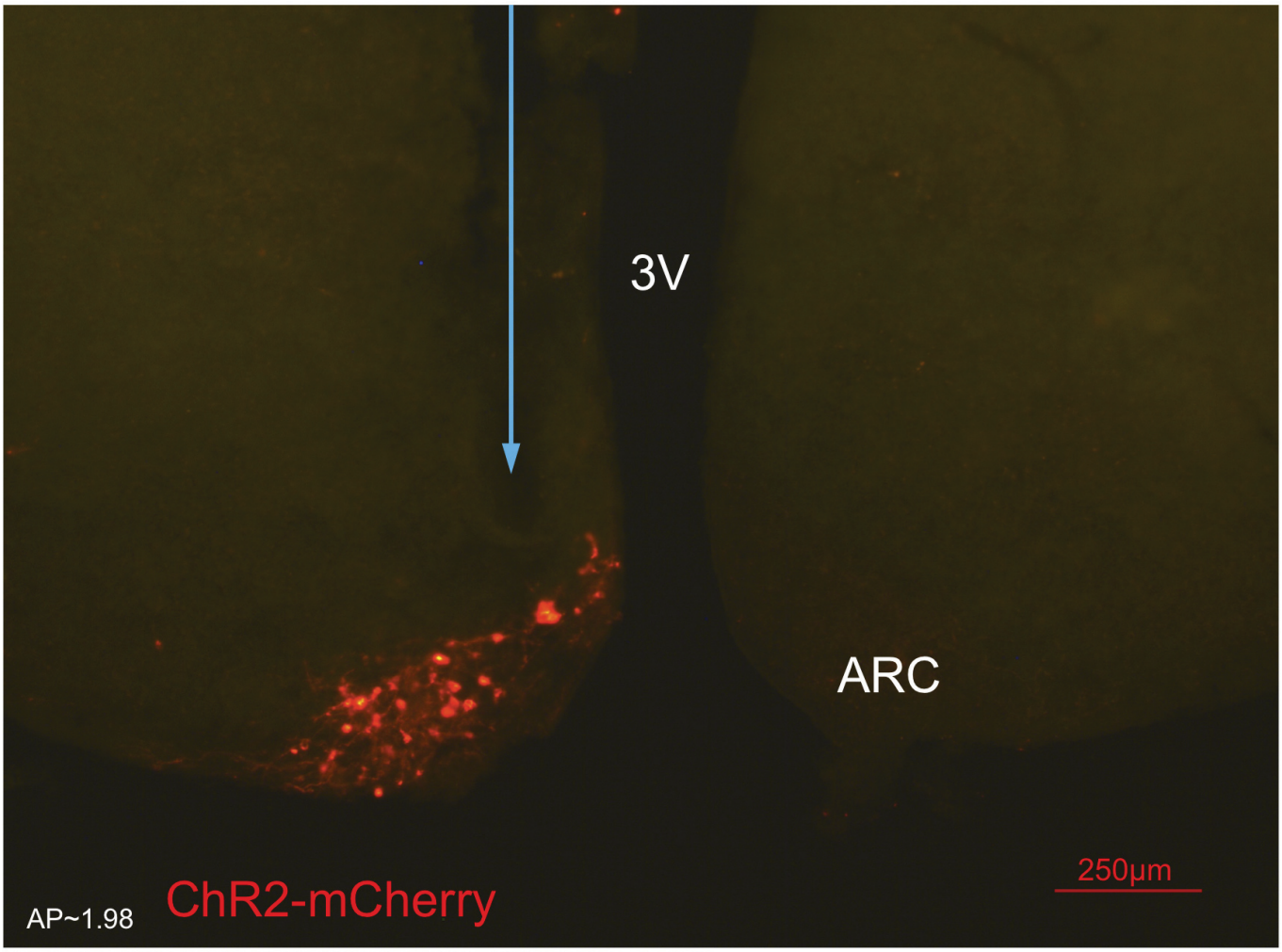

JNeurosci Accepted Manuscript

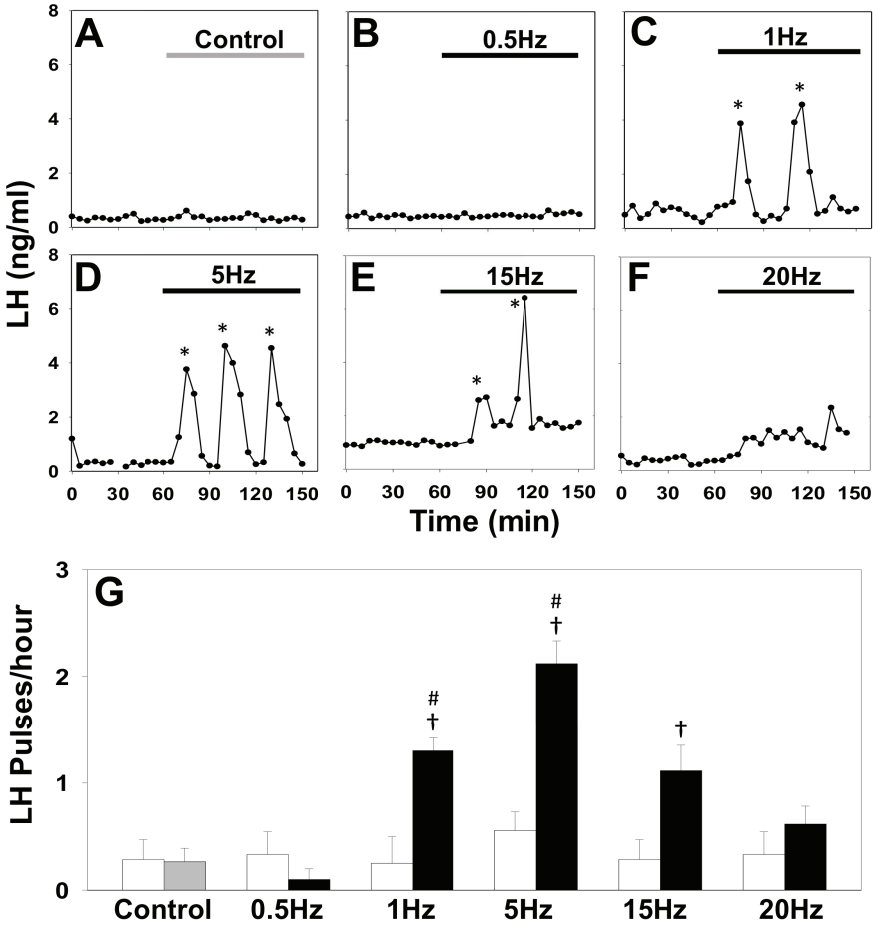

JNeurosci Accepted Manuscript

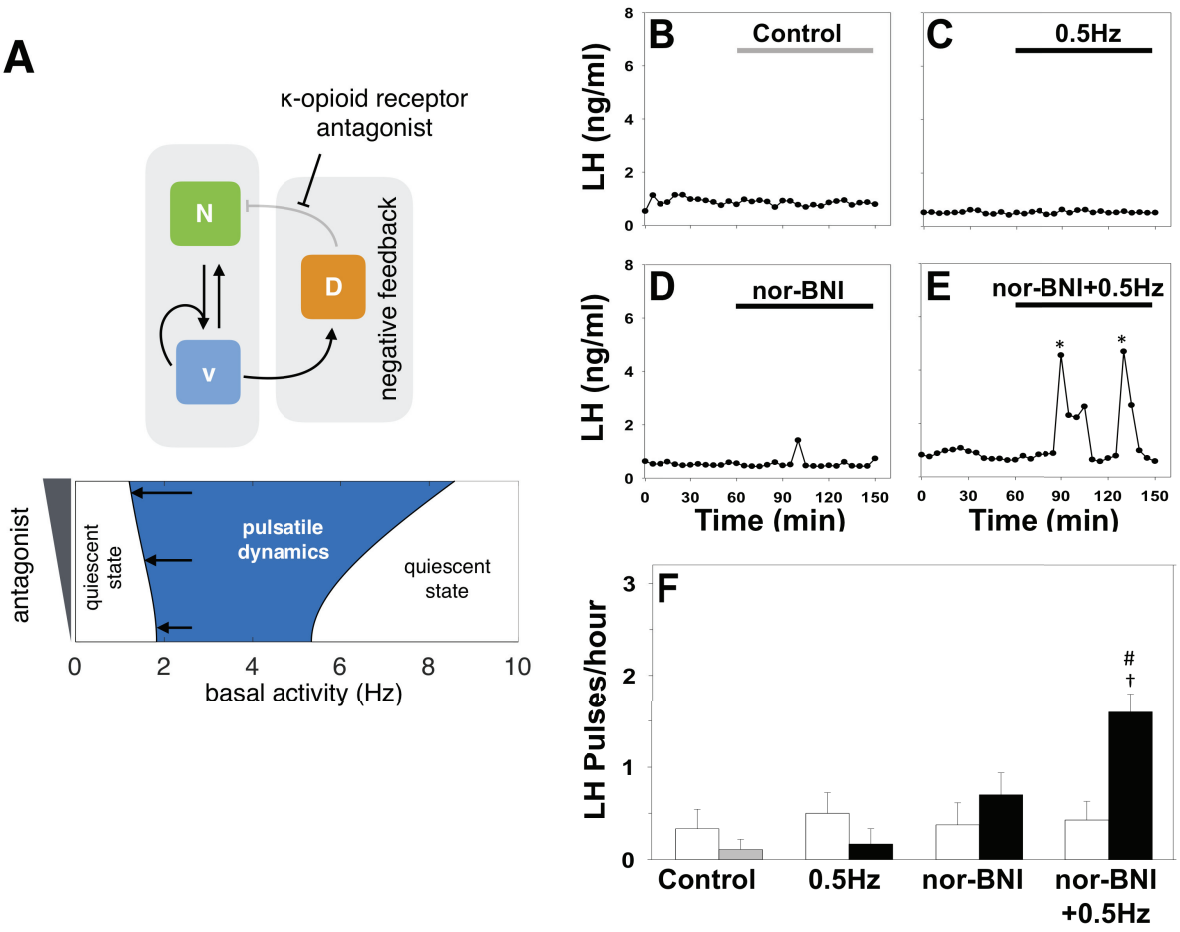

JNeurosci Accepted Manuscript

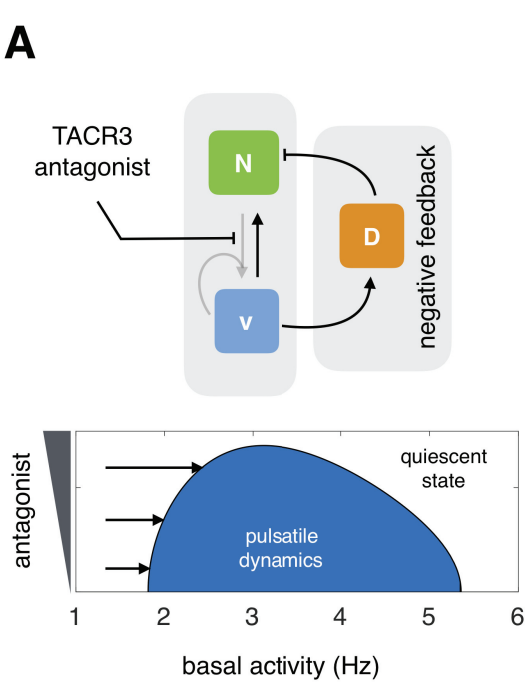

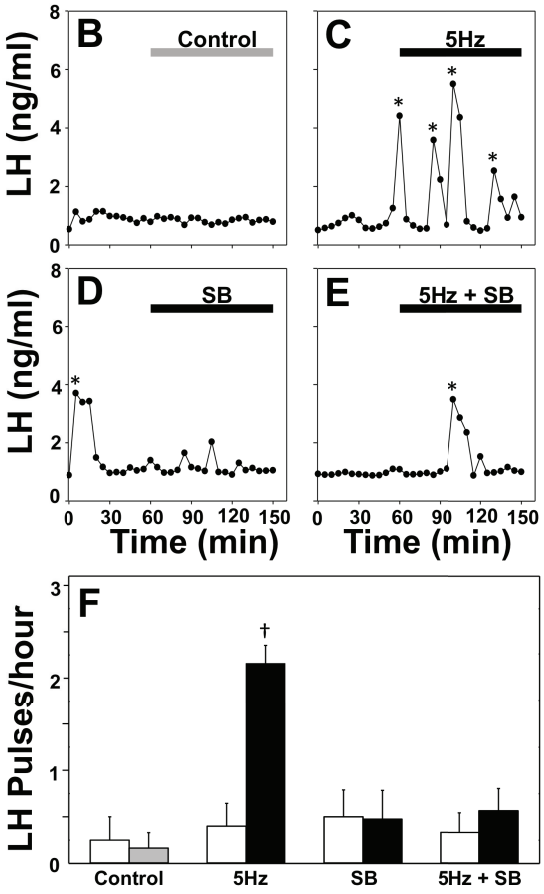

JNeurosci Accepted Manuscript